Bandwidth-Adaptive Single- and Double-Channel Silicon Photonic Contra-Directional Couplers

Mohammad Amin Mahdian[1], Lorenzo Tunesi[2], Paolo Bardella[2], and Mahdi Nikdast[1]
[1]Department of Electrical and Computer Engineering, Colorado State University, Fort Collins, CO 80523 USA
[2]Department of Electronics and Communications, Politecnico di Torino, Turin, Italy

***Abstract*—We present a detailed design-space exploration for silicon photonic contra-directional couplers (CDCs) with sub-wavelength and waveguide gratings, considering similar and different periods. Using this design exploration, we create adaptive bandwidth single- and double-channel CDCs controlled by thermal chirping in the optical C-band.**

I. Introduction

Contra-directional couplers (CDCs) have found widespread use in the design of flat-top add-drop filters and switches [1], [2]. However, these devices are subject to limited bandwidth, and the proposed solutions (e.g., [3], [4]) aimed at improving their bandwidth often lead to larger footprints while limiting their tunability. This is primarily attributed to the use of multiple CDCs in parallel or series configurations, which inevitably increases the overall size of the device [2]. Furthermore, the larger footprints impose limitations on achieving precise tuning and maintaining reasonable power consumption when utilizing thermal tuning mechanisms.

To address bandwidth tunability and response tailoring in CDCs, this paper presents a detailed design-space exploration and provides insights into the design and control of CDCs' bandwidth by investigating three different CDC designs: waveguide CDCs (W-CDCs), half subwavelength-grating (SWG) CDCs (HSWG-CDCs), and SWG-CDCs, all of which are depicted in Fig. 1. We also consider single and two periods in these structures. In the single-period configuration, both gratings have the same period, while in the two-period configuration, the two gratings have different periods. Moreover, we present a comprehensive analysis and evaluation of a C-band-specific HSWG-CDC. The investigated designs offer versatile single- or double-channel responses, with bandwidths ranging from a few nanometers to >30 nm.

II. Principle of Contra-Directional Couplers

CDCs are four-port devices capable of coupling light in the opposite direction into another waveguide, eliminating the need for optical circulators [2], [3]. A conventional CDC structure is depicted in Fig. 1(a). The gap distance in this paper refers to the distance between the two non-corrugated waveguides. The width of the narrower waveguide is denoted as W_1, and the width of the wider waveguide is shown as W_2. The different widths of the two waveguides are designed to suppress the directional coupling effect [3]. The protruding section of the corrugation is defined by $\Delta w_{max1,2}$, which adds up to the width of each waveguide. The period of each waveguide grating is denoted as Λ_1 and Λ_2, which can be the same or different in the case of a two-period design, resulting in two channels in the drop-port response, as we will show in Section III.

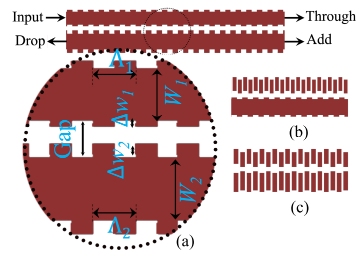

Fig. 1. Schematic of a (a) conventional waveguide-based CDC structure, (b) half subwavelength-grating CDC, and (c) subwavelength-grating CDC.

CDC's drop-port response exhibits significant sidelobes that restrict the device's bandwidth. As a solution, apodization techniques are deployed to improve the sidelobe suppression ratio (SLRL) [2], [4]. In apodized structures, the depth of the corrugations is modulated to avoid abrupt changes of the coupling along the length of the device. Gaussian and $\tanh$ are two extensively used apodization functions for CDCs.

There are various methods for controlling the bandwidth and the central wavelength of a CDC, including thermo-optic and electro-optic tuning [2], [3], each with some benefits and drawbacks. The designs discussed in this paper are tuned using thermo-optic microheaters.

III. Bandwidth-Adaptive Single- and Double-Channel CDCs: Design and Results

We investigate the design of the three CDC structures demonstrated in Fig. 1. In all these three designs, waveguides have widths of $W_1 = 560$ nm and $W_2 = 440$ nm, and are positioned in close proximity to each other at a 200-nm gap. In the SWG-based structures, the duty cycle is considered to be 70%. The average index of the structure in SWG-CDC and HSWG-CDC is lower compared to the W-CDC, which necessitates different grating periods in various CDC designs.

The bandwidth of the CDC is directly impacted by Δw_{max}. In two-period CDCs, adjusting Δw_{max} for the two waveguides allows independent tuning of the bandwidth for each channel. All designs are apodized using the $\tanh$ function:

$$\Delta w\left(n\right) = \frac{\Delta w_{max}}{2}\left[1 + tanh\left(\beta\left(1 - 2\left|\frac{2n-N}{N}\right|^{\alpha}\right)\right)\right]. \quad (1)$$

Here, n and N are the number and the total number of the gratings, respectively. The apodization parameters α and β are

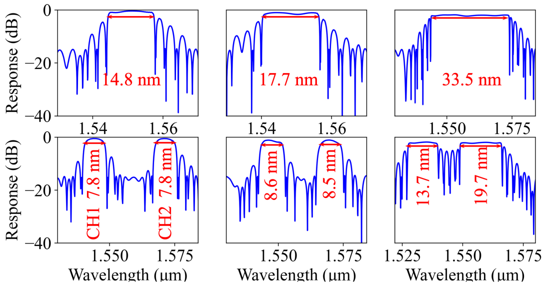

Fig. 2. Drop-port response for (from top left to bottom right): single-period W-CDC, HSWG-CDC, and SWG-CDC; and two-period W-CDC, HSWG-CDC, and SWG-CDC. 3-dB bandwidth is noted in red.

constants, assumed to be 2 and 5 in our designs. Assuming approximately $N = 1200$ gratings, increasing the period can enhance the coupling coefficient of crosstalk in CDC.

In the two-period CDC setup, a 2 nm or greater difference in grating periods can create two separate channels in the drop-port response. The operational intricacies of these devices are extensively discussed in [5]. In the two-period SWG-CDC configuration, the drop-port response demonstrates a wideband characteristic, exceeding 30 nm for each channel. However, accommodating two wideband channels within the C-band proves to be challenging. Additionally, the wideband reflection from the through port on the input port can easily disrupt the response of the other channel's response at the through port, further complicating the design.

We designed three different CDCs with two different configurations, including single- and two-period W-CDCs, HSWG-CDCs, and SWG-CDCs. Fig. 2 shows the spectral drop-port response for these different designs. We place our primary focus on optimizing the bandwidth of the drop port by employing thermal chirping and apodization techniques. Among the responses shown, SWG-CDC exhibits the highest bandwidth in both single-period and two-period configurations, surpassing 30 nm. This is due to the higher contra-directional coupling coefficient when using SWGs, compared to conventional W-CDCs. By increasing the duty cycle of the gratings, it is possible to further enhance the bandwidth of the CDC's drop-port response. Similarly, the HSWG-CDC structure also exhibits a higher bandwidth exceeding 20 nm when compared to the conventional design.

In Fig. 3(a), the bandwidth performance of the three designs are compared for a single-period configuration, employing six different levels of linear thermal chirping. This chirping is achieved by utilizing segmented heaters, enabling the creation of arbitrary temperature profiles along the CDC [2] to enhance the bandwidth. In comparing the passive response of the three devices, SWG-CDCs offer the highest bandwidth, followed by HSWG-CDC and W-CDC designs. All three designs have similar parameters except for the adjusted period to accommodate channels within C-band. The initial temperature is set at 300 K, with ΔT representing the linearly increasing temperature difference over 20 steps.

To investigate the thermal-chirp effect, designs are tested using FDTD simulations and validated with a mathematical

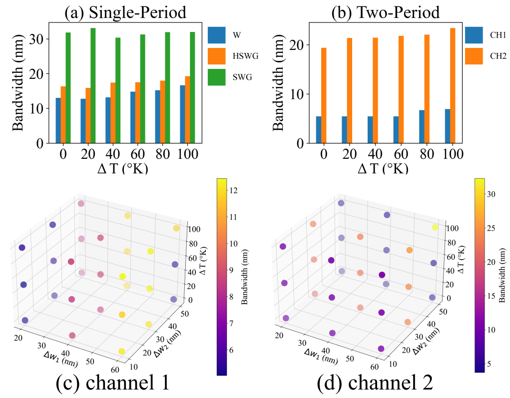

Fig. 3. (a) Bandwidth comparison among the three different designs with single-period configuration under different thermal-chirp conditions. (b) Effect of thermal chirping on the bandwidth of a two-period HSWG-CDC. (c) and (d): $\Delta w_{max1,2}$ effect of thermal chirping on the bandwidth of an HSWG-CDC on the two channels.

model provided in [3]. Thermal chirping has the greatest impact on W-CDC and HSWG-CDC structures. For these designs, the bandwidth (considering single-period) can increase by up to 28% and 18%, respectively, when thermally chirped from 300 to 400 K. In Fig. 3(b), the effect of thermal chirping is demonstrated for an imbalanced two-period HSW-CDC design (periods: 340 and 346 nm). The bandwidth of the channels can be controlled by carefully adjusting $\Delta w_{max1,2}$. In the passive design, the bandwidth of the first and second channels is 5.43 and 19.38 nm, respectively. Thermal chirping has the most significant effect on the second channel, increasing its bandwidth by up to 4 nm when the device is linearly chirped from 300 to 400 K.

Figs. 3(c) and 3(d) show how different $\Delta w_{max1,2}$ values impact the bandwidth of an HSWG-CDC under different thermal-chirp conditions. Note that having a larger Δw_{max} on the SWG waveguide creates a balanced bandwidth between the two channels. The highest bandwidth for both channels occurred when $\Delta w_{max1,2}$ were set to 60 (SWG-CDC) and 50 (W-CDC), respectively. In this configuration, channel 1 achieved a bandwidth of 11.72 nm, while channel 2 exhibited a bandwidth of 32.29 nm which is comparable to that of the SWG-CDC. In addition, HSWG-CDCs offer similar performance in a shorter length compared to conventional designs due to their stronger contra-directional coupling coefficients.

In summary, this paper explored different CDC designs and their bandwidth performance. The HSWG-CDC design offers a versatile response in both single- and two-period configurations. The two-period designs are beneficial for applications needing two distinct channels. By utilizing a two-period CDC, it is possible to achieve a comparable response to cascaded designs in a shorter length, thanks to the nonlinear properties of the two-period grating structures.

References

[1] H. Qiu *et al.*, *Journal of Lightwave Technology*, vol. 36, no. 17, 2018.
[2] J. Cauchon *et al.*, *Optics Letters*, vol. 46, no. 3, pp. 532–535, 2021.
[3] W. Shi *et al.*, *Optics express*, vol. 21, no. 3, pp. 3633–3650, 2013.
[4] M. Hammood *et al.*, *Optics Letters*, vol. 46, no. 11, 2021.
[5] M. Boroojerdi *et al.*, *Optics Express*, vol. 24, no. 20, 2016.

This work was supported by the NSF under grants CNS-2046226 and CCF-2006788.